Stabilizing the VE-cadherin–catenin complex blocks leukocyte extravasation and vascular permeability

Dörte Schulte[1], Verena Küppers[1], Nina Dartsch[1], Andre Broermann[1], Hang Li[1], Alexander Zarbock[1,2], Olena Kamenyeva[1], Friedemann Kiefer[1], Alexander Khandoga[3], Steffen Massberg[3] and Dietmar Vestweber[1,*]

[1]Department of Vascular Cell Biology, Max-Planck-Institute of Molecular Biomedicine, Münster, Germany, [2]Department of Anesthesiology and Critical Care Medicine, University of Münster, Münster, Germany and [3]ISARESEARCH Center, German Heart Center Munich, University of Munich, Munich, Germany

To determine whether leukocytes need to open endothelial cell contacts during extravasation, we decided to generate mice with strongly stabilized endothelial junctions. To this end, we replaced VE-cadherin genetically by a VE-cadherin–α-catenin fusion construct. Such mice were completely resistant to the induction of vascular leaks by VEGF or histamine. Neutrophil or lymphocyte recruitment into inflamed cremaster, lung and skin were strongly inhibited in these mice, documenting the importance of the junctional route *in vivo*. Surprisingly, lymphocyte homing into lymph nodes was not inhibited. VE-cadherin–α-catenin associated more intensely with the actin cytoskeleton as demonstrated by its membrane mobility and detergent extractability. Our results establish the junctional route as the main pathway for extravasating leukocytes in several, although not in all tissues. Furthermore, in these tissues, plasticity of the VE-cadherin–catenin complex is central for the leukocyte diapedesis mechanism.

Introduction

The entry of leukocytes from the blood stream into tissue initiates the immune defense at sites of inflammation and represents the basis of lymphocyte homing during immune surveillance. Whereas the mechanisms that initiate and mediate leukocyte endothelial contact formation are very well studied (Ley *et al*, 2007), it is less well understood how leukocytes actually migrate through the blood vessel wall, a process called diapedesis (Muller, 2003; Vestweber, 2007; Nourshargh *et al*, 2010). Leukocytes can exit the blood stream either by migration through the junctions between endothelial cells (paracellular) or by transcytosis through the body of single endothelial cells (transcellular). Each of these two pathways has been documented by transmission electron microscopy in numerous studies; however, only few have thoroughly analysed serial sections through each extravasating leukocyte, which is absolutely necessary to exclude misinterpretation of the route a leukocyte takes. Unfortunately, even such thorough studies support contradictory conclusions either claiming that leukocytes use exclusively the paracellular diapedesis route (Marchesi, 1961; Schoefl, 1972; Anderson and Anderson, 1976), or exit exclusively via the transcellular route (Marchesi and Gowans, 1964; Farr and DeBruyn, 1975; Feng *et al*, 1998; Hoshi and Ushiki, 1999). Since it is extremely tedious to generate a sufficient number of serial sections to cover the whole body of an extravasating leukocyte, each of these studies only analysed the diapedesis route of a rather limited number of single leukocytes. Thus, it is difficult to make quantitative statements that allow to conclude whether the majority of extravasating leukocytes in a given tissue, or for a given inflammatory stimulus take the transcellular route or the junctional route and it is presently unclear whether these routes are of equal physiological relevance or whether one of them prevails.

Confocal microscopy of *in vitro* diapedesis revealed that only 5–11% of neutrophils, monocytes or lymphocytes migrate through HUVEC monolayers via the transcellular route (Carman and Springer, 2004). However, the use of microvascular endothelial cells in these assays increased the percentage of transcellularly migrating leukocytes up to 30% (Carman *et al*, 2007). Peripheral blood mononuclear cells (mainly T and B cells) were even reported to migrate mostly through the transcellular route, if they were incubated with HUVEC monolayers under flow conditions, whereas neutrophils migrated exclusively through junctions under these conditions (Nieminen *et al*, 2006). Thus *in vitro*, the type of assay system employed apparently affects the transmigration route.

To determine *in vivo* whether and to what extent the junctional diapedesis route is of physiological relevance for the extravasation of leukocytes, we decided to block specifically the junctional pathway in gene-targeted mice. We based our approach on the assumption that leukocytes extravasating through the paracellular pathway would need to destabilize VE-cadherin-mediated cell adhesion. VE-cadherin is known to mediate stability of endothelial cell contacts *in vivo* since adhesion-blocking antibodies enhance vascular permeability (Corada *et al*, 1999) and leukocyte extravasation (Gotsch *et al*, 1997). Thus, stabilizing the adhesive function of VE-cadherin should create endothelial

*Corresponding author. Department of Vascular Cell Biology, Max-Planck-Institute of Molecular Biomedicine, Roentgenstr. 20, Münster 48149, Germany. Tel.: +49 251 70365 210/200 Secr.; Fax: +49 251 70365 299; E-mail: vestweb@mpi-muenster.mpg.de

junctions that would resist opening. If this were the case, this approach should allow us to test whether and to what extent opening of endothelial cell contacts, and thus the paracellular pathway would contribute to leukocyte extravasation. In addition, if stabilizing the adhesive function of VE-cadherin blocked leukocyte extravasation, this would establish for the first time, that downregulation of VE-cadherin adhesive activity is indeed an essential step in leukocyte extravasation *in vivo*.

Cadherins are known to associate with the intracellular catenins by directly binding to β-catenin that forms the link to α-catenin (Kemler, 1993). This association is essential for stable cadherin-mediated adhesion (Ozawa *et al*, 1989; Hirano *et al*, 1992). In agreement with this, an E-cadherin–α-catenin fusion protein supported cell adhesion much more stably than E-cadherin when expressed ectopically in cells devoid of endogenous cadherins (Nagafuchi *et al*, 1994; Ozawa and Kemler, 1998).

Here, we have generated gene-targeted mice by replacing VE-cadherin by a VE-cadherin–α-catenin fusion protein. These mice were completely resistant to strong vascular permeability-inducing factors such as VEGF and histamine, demonstrating that we have generated mice with highly stabilized endothelial junctions. Investigating leukocyte extravasation in various inflammation models revealed a dramatic block of the extravasation of leukocytes in several tissues demonstrating the importance of the paracellular diapedesis route. Furthermore, our results show that the plasticity of the VE-cadherin–catenin complex, most likely via modifying the interaction with the actin cytoskeleton, is essential for the induction of vascular permeability and leukocyte extravasation *in vivo*.

Results

Generation and characterization of gene-targeted mice expressing VE-cadherin–α-catenin instead of VE-cadherin

In order to generate mice with stabilized endothelial cell contacts, we targeted the VE-cadherin (*Cdh5*) gene locus with a VE-cadherin–α-catenin (VEC–α-C) construct in such a way that the translational start ATG of the fusion construct replaced the corresponding ATG of the VE-cadherin gene. A transcriptional stop signal at the 3′ end of the cDNA construct prevented transcription of down stream VE-cadherin exons (Figure 1A). For controls, additional knock-in mice were generated in the same way by targeting the VE-cadherin locus with WT VE-cadherin cDNA (VEC–WT). For all assays performed throughout this study, WT mice and VEC–WT mice were indistinguishable (not shown).

The VEC–α-C fusion protein consisted of a truncated form of VE-cadherin lacking the β-catenin binding site (C-terminal 75 aa), which was fused to the C-terminal part (aa 301–900) of α-catenin (Figure 1B). Heterozygous mice ($+$/VEC–α-C) were viable and born at Mendelian frequency, whereas VEC–α-C homozygous mice were underrepresented when
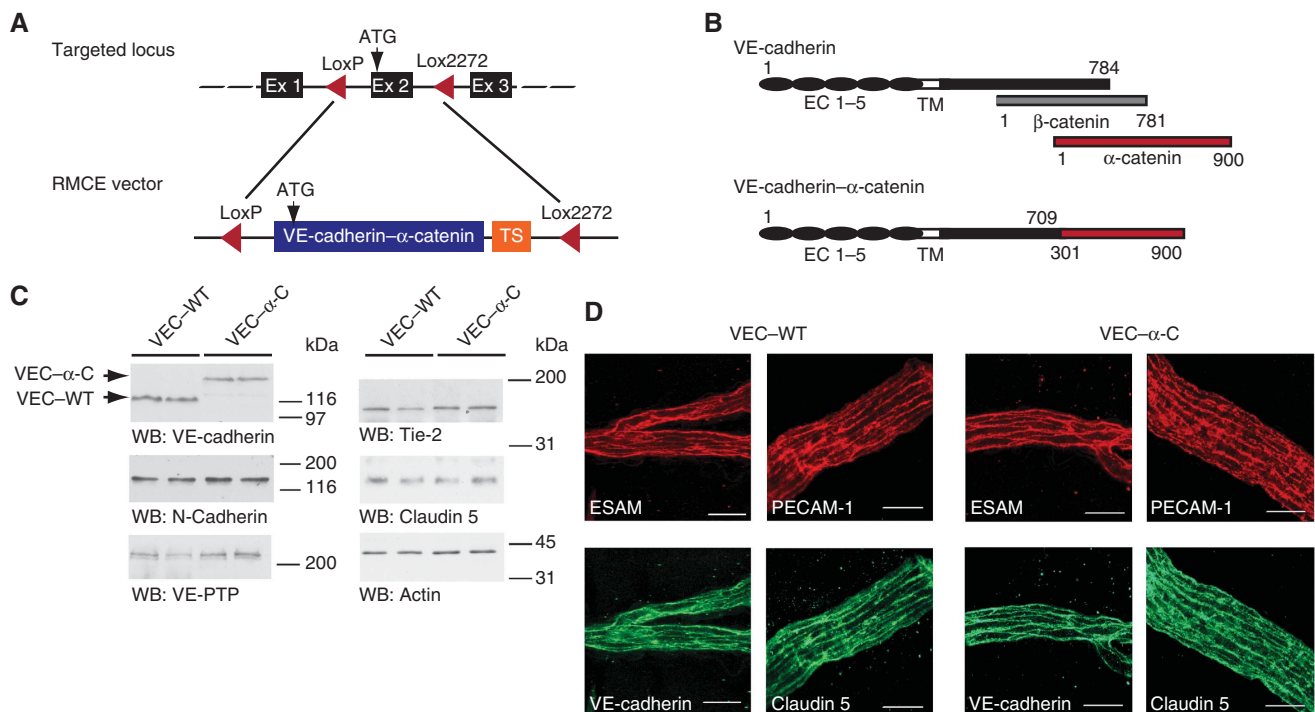

Figure 1 Generation of VE-cadherin–α-catenin knock-in mice. (**A**) Schematic illustration of targeting exon 2 (Ex2) of the VE-cadherin locus by recombinase-mediated cassette exchange (RMCE). Two incompatible LoxP sites (LoxP and Lox2272) were positioned to flank exon 2 in order to replace this exon in a second step with a replacement cassette flanked with the same Lox sites and containing VEC–α-C cDNA followed by a polyA-transcriptional stop (TS) cassette. (**B**) Schematic illustration of VE-cadherin, β-catenin, α-catenin and the VEC–α-C fusion protein depicting the extracellular (EC 1–5) and transmembrane (TM) domains of VE-cadherin. Numbers refer to amino-acid positions. (**C**) Western blot (WB) of SDS-urea extracts of lung tissue of homozygous adult VEC–WT and VEC–α-C mice, immunoblotted for VE-cadherin, N-cadherin, VE-PTP, Tie-2, claudin 5 and actin. Molecular weight markers are indicated on the right. Results of two mice for each genotype are shown. (**D**) Whole-mount stainings of cremaster muscles from VEC–WT and VEC–α-C mice using antibodies against VE-cadherin, ESAM, PECAM-1 and claudin 5. Projections of z-stacks taken on an LSM 510 Zeiss Meta, bars = 20 μm. Figure source data can be found with the Supplementary Information.

+/VEC–α-C mice were crossed (4% instead of 25%) and when heterozygous mice were mated with VEC–α-C homozygous mice (14% instead of 50%) (Supplementary Table S1). Breeding of homozygous mutant mice resulted in 40–50% of viable pups compared with matings of VEC–WT mice of similar genetic background. These results were obtained on a mixed 129SV × C57Bl/6 genetic background. Backcrossing to the C57Bl/6 strain resulted in 100% embryonic lethality of homozygous mutant mice (as determined for sixth backcross). The developmental defects leading to embryonic lethality will be analysed in future studies. Viable mice of homozygous mutant genotype showed no obvious phenotype and were healthy and fertile when housed under special pathogen-free conditions.

The VEC–α-C fusion protein was expressed in homozygous mutant mice at slightly reduced levels compared with VE-cadherin in VEC–WT mice, as determined by western blot analysis of lung homogenates (Figure 1C). The expression levels of membrane proteins relevant for endothelial cell contacts such as VE-PTP, Tie-2 and claudin 5 and also the expression of N-cadherin were unaffected in mutant mice (Figure 1C). As shown in Figure 1D, whole-mount stainings of cremaster tissue revealed normal subcellular distribution of claudin 5, ESAM, PECAM and the VEC–α-C fusion protein at endothelial cell contacts in venules of homozygous mutant mice. Analysing peripheral leukocyte counts revealed that the number of all leukocytes and neutrophils were elevated by 50% in VEC–α-C mice compared with VEC–WT mice (Supplementary Table S2). This was not due to differences in haematopoiesis since leukocyte populations in the bone marrow were similar in both types of mice (Supplementary Table S3).

VE-cadherin–α-catenin blocks induction of vascular permeability by VEGF and histamine

To test whether VEC–α-C indeed stabilizes endothelial cell contacts *in vivo*, we analysed the induction of vascular permeability in VEC–α-C mice. Using the Miles assay, we found that local injection of VEGF into the skin of VEC–WT mice that had been injected i.v. with Evans Blue induced strong leakiness of the dye within 30 min, whereas VEC–α-C mice were completely resistant and showed no leakiness (Figure 2A). A similar result was found for challenging the

mice with histamine (Figure 2B). Thus, VEC–α-C indeed locked endothelial junctions in the skin and made them resistant to opening by VEGF or histamine.

VE-cadherin–α-catenin strongly reduces extravasation of leukocytes in IL-1β inflamed cremaster

Since VEC–α-C blocked the opening of endothelial junctions in the Miles assay, we tested whether this would affect the extravasation of neutrophils in inflamed cremaster tissue. Two different methods were used to analyse this. Three hours after intrascrotal injection of IL-1β, the cremaster was prepared, fixed and whole mounts were stained for PECAM-1 to visualize endothelial cell contacts and for MRP-14 to mark neutrophils. Whole mounts were analysed by confocal microscopy to distinguish and quantify leukocytes inside and outside blood vessels. This analysis revealed a 74% (± 5.8%) reduction in the number of neutrophils extravasated in VEC–α-C mice in comparison with VEC–WT mice (Figure 3B). As a second method, we used intravital microscopy to directly observe leukocyte extravasation after 4 h of stimulation with IL-1β. We found that neutrophil extravasation was reduced by 67% (± 2%), whereas adhesion and rolling were not affected (Figure 3C–F). These results suggest that stabilization of endothelial junctions inhibits diapedesis of most of the extravasating neutrophils in the IL-1β inflamed cremaster.

Recruitment of neutrophils or lymphocytes into inflamed lung or skin of VE-cadherin–α-catenin mice is strongly reduced

To test whether VEC–α-C would also reduce leukocyte recruitment in other tissues, we analysed two more inflammation models. We challenged the lungs of mice for 30 min with LPS and after 4 h the number of intravascular and extravascular neutrophils was determined as described (Zarbock *et al*, 2008). Again we found that neutrophil extravasation was reduced by 63% (± 8.5%) in VEC–α-C mice when compared with VEC–WT mice (Figure 4A). Thus, despite major differences between the molecular mechanisms of leukocyte extravasation between lung and cremaster tissue, in both tissues the opening of endothelial junctions is necessary for extravasation of the majority of recruited neutrophils.

As a third inflammation model, we tested the hapten-induced entry of activated lymphocytes into the skin in a delayed type hypersensitivity (DTH) reaction. As shown in Figure 4B, dinitrofluorbenzene (DNFB)-elicited emigration of [51Cr]-labelled activated T cells into the skin at 5 h after injection was reduced by 57% (± 6.2%) in VEC–α-C mice when compared with VEC–WT mice. We conclude that not only neutrophils, but also activated T lymphocytes use the junctional diapedesis pathway for efficient extravasation.

VE-cadherin–α-catenin does not impair homing of naive lymphocytes into lymph nodes

The increased peripheral leukocyte counts (Supplementary Table S2) prompted us to determine the number of lymphocytes in lymph nodes and spleen. Unexpectedly, the numbers were not significantly different between VEC–WT and VEC–α-C mice (Supplementary Tables S4 and S5). Analysing short-term lymphocyte homing, we injected primary isolated [51Cr]-labelled naive lymphocytes from lymph nodes of VEC–WT mice into VEC–WT and VEC–α-C mice and determined the accumulation of radioactivity in peripheral lymph
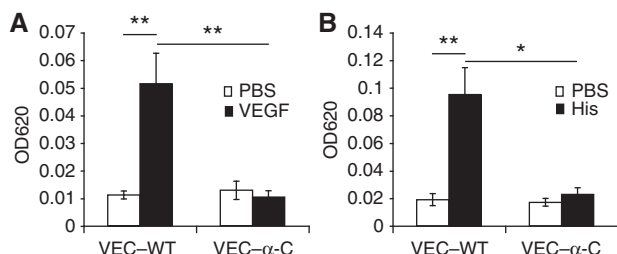

Figure 2 VE-cadherin–α-catenin blocks VEGF and histamine-induced permeability *in vivo*. VEC–WT and VEC–α-C mice were intravenously injected with Evans Blue and 10 min later intradermally with PBS for controls (open bars) and either VEGF (**A**) or histamine (**B**) (black bars). Thirty minutes later, skin areas were excised and the dye was extracted and quantified. One representative experiment out of three independent experiments with at least four mice per group is shown. *$P \leqslant 0.05$; **$P \leqslant 0.01$; (**A**) *t*-test; (**B**) Mann rank Sum Test.
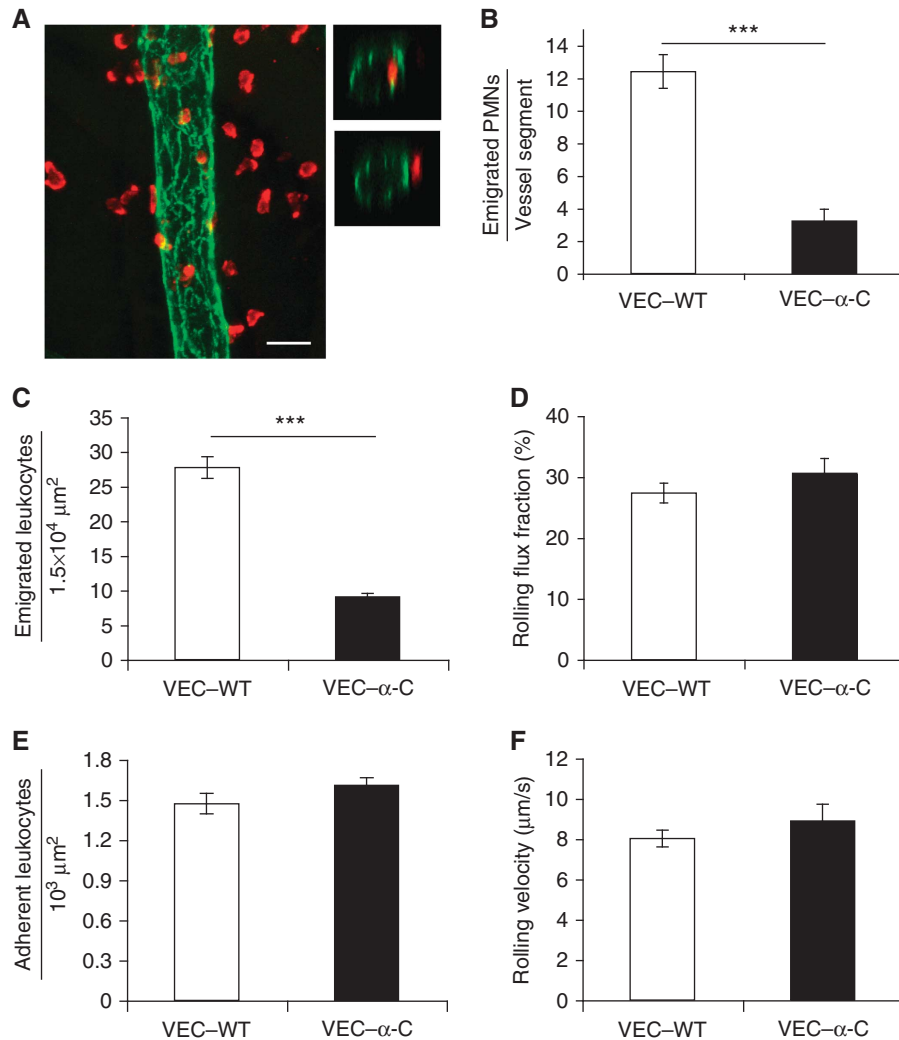
Figure 3 Extravasation of leukocytes into IL-1β-stimulated cremaster muscle is strongly reduced in VE-cadherin–α-catenin mice. (**A**, **B**) Confocal fluorescence microscopy was used to determine the number of extravasated neutrophils 3 h after intrascrotal IL-1β injection. (**A**) Representative images of whole mount stainings of cremaster labelled for PECAM-1 (green) and MRP-14 (red) to visualize endothelial cell contacts and neutrophils, respectively. Left panel: longitudinal vessel segment typically used for the 3D analysis and evaluation. Right panels: optical cross-sections of a venule depicting a neutrophil inside (upper right panel) and outside (lower right panel) the vessel. Projections of z-stacks taken on an LSM Zeiss 510 Meta, bar = 20 μm. (**B**) Numbers of extravasated neutrophils in VEC–WT and VEC–α-C mice located within 50 μm next to the vessel were counted and are given per vessel segment (length 150 μm). A total of 60 (VEC–WT) and 66 (VEC–α-C) vessel segments from three mice of each group were analysed. (**C–F**) Intravital microscopy of neutrophil extravasation in venules of the cremaster muscle 4 h after intrascrotal administration of IL-1β. (**C**) Numbers of extravasated leukocytes in cremaster venules of VEC–WT and VEC–α-C mice per 1.5×10^4 μm² tissue area determined by reflected light oblique transillumination microscopy. (**D**) Rolling flux fraction, (**E**) number of adhering leukocytes per 10^3 μm² of venule surface area, (**F**) rolling velocity. A total of 28 or 35 vessels from 4 VEC–WT and 5 VEC–α-C mice were analysed. Haemodynamic parameters are given in Supplementary Table S6, showing that peripheral neutrophil counts, enhanced under inflammatory conditions, were similar in VEC–WT and VEC–α-C mice. ***$P \leqslant 0.001$; Mann Rank Sum Test.

nodes (PLN) and mesenteric lymph nodes (MLN) 3 h later. Surprisingly, and in strong contrast to our results in three different inflamed tissues, VEC–α-C did not impair the accumulation of naive lymphocytes in lymph node tissue (Figure 4C). Thus, diapedesis of naive lymphocytes through high endothelial venules (HEVs) of lymph nodes differs fundamentally from leukocyte extravasation into various inflamed tissues.

VE-cadherin–α-catenin blocks only paracellular but not transcellular diapedesis

The striking efficiency with which VEC–α-C blocked the opening of endothelial junctions strongly suggested that this is also the reason why the covalent fusion of VE-cadherin

with α-catenin inhibits leukocyte extravasation. To directly determine whether indeed only paracellular but not transcellular diapedesis is affected by this fusion protein, we expressed either VEC–α-C–GFP or VEC–GFP in HUVEC cells and analysed transmigration of granulocytic-HL60 cells through monolayers of these cells grown on coverslips. VEC–α-C–GFP was always expressed at slightly reduced levels than VEC–GFP at cell contacts, ensuring that inhibitory effects of VEC–α-C–GFP on transmigration were not due to stronger expression levels (Figure 5C). Paracellular and transcellular migration of leukocytes were determined as described (Carman and Springer, 2004) defining the point of leukocyte penetration through the endothelium as the area being devoid of ICAM-1 fluorescence. Typical examples for
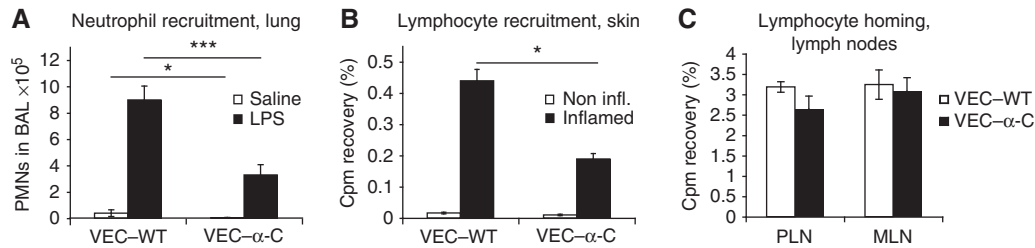
Figure 4 VE-cadherin–α-catenin strongly reduces extravasation of neutrophils or lymphocytes into inflamed lung or skin, but not lymphocyte homing. (**A**) LPS induced PMN recruitment into inflamed lungs. The number of neutrophils in the bronchoalveolar lavage (BAL) of VEC–WT and VEC–α-C mice was analysed using flow cytometry 4 h after inhalation of LPS (black bars) or NaCl (open bars). Four mice were analysed per group. (**B**) DTH response in the skin was analysed by injection of radiolabelled, *in vivo*-activated lymphocytes from VEC–WT mice into DNFB-sensitized VEC–WT and VEC–α-C mice. Immigration of cells into the non-inflamed control ears (open bars) and inflamed ears (black bars) was analysed 5 h after lymphocyte injection. The depicted experiment was performed with six VEC–WT and four VEC–α-C mice and is representative of two separate experiments. (**C**) Radiolabelled naive lymphocytes from VEC–WT mice were injected intravenously into VEC–WT and VEC–α-C mice and the percentage of the total injected radioactivity in peripheral lymph nodes (PLN) and mesenteric lymph nodes (MLN) was determined 3 h later; $n = 5$ (VEC–WT) and $n = 6$ (VEC–α-C). One representative experiment out of two independent experiments is shown. $*P \leqslant 0.05$; $***P \leqslant 0.001$, t-test.

transcellularly and paracellularly migrating leukocytes are illustrated in Figure 5B. Quantifying our results, we found that paracellular migration was inhibited by the cadherin–catenin fusion protein by 46% ($\pm 13.8\%$), whereas transcellular migration was not significantly inhibited (Figure 5A), demonstrating that the inhibitory effect of VEC–α-C on transmigration selectively affects the junctional diapedesis route. Transmigration of mouse PMNs through endothelioma cells established from VEC–α-C mice was inhibited by 45% when compared with endothelioma cells from VEC–WT mice (Figure 5E). Expression levels of various adhesion molecules were similar on these endothelioma cells, and were also similar on endothelial cells isolated from cremaster tissue of both types of mice (Supplementary Figure S1).

To rule out that the deletion of the C-terminal 75 amino acids of VE-cadherin in our VEC–α-C–GFP fusion protein would be responsible for the inhibitory effect on transmigration we generated a similar fusion protein with full-length VE-cadherin (VECfl–α-C–GFP). As shown in Figure 5D, expression of both fusion proteins via adenoviral vectors in HUVEC inhibited transmigration of granulocytic-HL60 cells to the same extent when compared with VEC–GFP. We conclude that the deletion of the β-catenin binding site in VEC–α-C is irrelevant for the inhibitory effect of this fusion protein on diapedesis. Expression levels of all three fusion proteins were similar (not shown).

VEGFR-2 signalling and VE-PTP association are not affected by VE-cadherin–α-catenin
VE-cadherin has been shown to modulate signalling via the VEGR-2 by associating with the receptor and interfering with its uptake into the cell (Lampugnani *et al*, 2006). Analysing whether VEC–α-C can still associate with VEGFR-2, we found that VEC–α-C was efficiently co-precipitated with the VEGFR-2 from endothelioma cells established from VEC–α-C mice (Figure 6A). Co-precipitated amounts were slightly reduced compared with co-precipitated VE-cadherin in endothelioma cells from VEC–WT mice due to reduced detergent extractability of VEC–α-C (Figure 6A and see below). Analysing VEGF signalling in these cells, we found that tyrosine phosphorylation of the VEGFR-2 and Erk1/2 induced by VEGF was similar in both types of cells (Figure 6B and C). We conclude, that signalling by VEGFR-2 is unaffected by the VEC–α-C fusion protein.

We described recently that VE-cadherin associates with the receptor type tyrosine phosphatase VE-PTP, which supports its adhesive function (Nottebaum *et al*, 2008). We found that the fusion between VE-cadherin and α-catenin did not affect the association with VE-PTP, since the ratio of VE-PTP immunoprecipitated from VEC–WT or from VEC–α-C endothelioma cells and co-precipitated VE-cadherin or VE-cadherin–α-catenin were similar (Figure 6D). In addition, in triple transfected COS cells, VE-PTP dephosphorylated Flk1-phosphorylated VE-cadherin as well as Flk1-phosphorylated VE-cadherin–α-catenin (Figure 6E).

Wnt signalling, cytoskeletal organization and endocytosis of VE-cadherin are not affected by VE-cadherin–α-catenin
We compared the expression levels of the catenins in VEC–WT and VEC–α-C mice by immunoblotting cell lysates. Since VE-cadherin–α-catenin does not bind to and thereby stabilize free α- and β-catenin or plakoglobin, expression levels of these catenins were lower in VEC–α-C cells (Figure 7A), although clearly detectable. p120 expression levels were unaltered (Figure 7A). Cytosolic or nuclear pools of β-catenin were not visible by immunofluorescence in both types of cells (Figure 7B); however, incubation with wnt3a for 14 h induced well-detectable nuclear β-catenin staining of similar intensity in VEC–WT and VEC–α-C cells (Figure 7B and C). Thus, the free β-catenin pool is not affected by the VE-cadherin–α-catenin fusion protein. Similarly, we found no difference in the ratio between the staining signals for VE-cadherin and α-catenin at cell contacts of VEC–WT or VEC–α-C cells (Figure 7D).

To determine, whether the VE-cadherin–α-catenin fusion protein would alter the formation of cortical actin or of vimentin filaments we stained VEC–WT and VEC–α-C endothelioma cells for these structures. As shown in Figure 8A, no differences were found. Furthermore, the phosphorylation/activation levels of myosin light chain were similar in these cells (Figure 8B) and also the ratio of F- to G-actin was indistinguishable (Figure 8C). These results indicate that the cytoskeletal organization is not altered in VEC–α-C cells.

Finally, we analysed whether VE-cadherin–α-catenin would be endocytosed with different efficiencies than VE-cadherin. We found that the same amounts of VEC–WT and
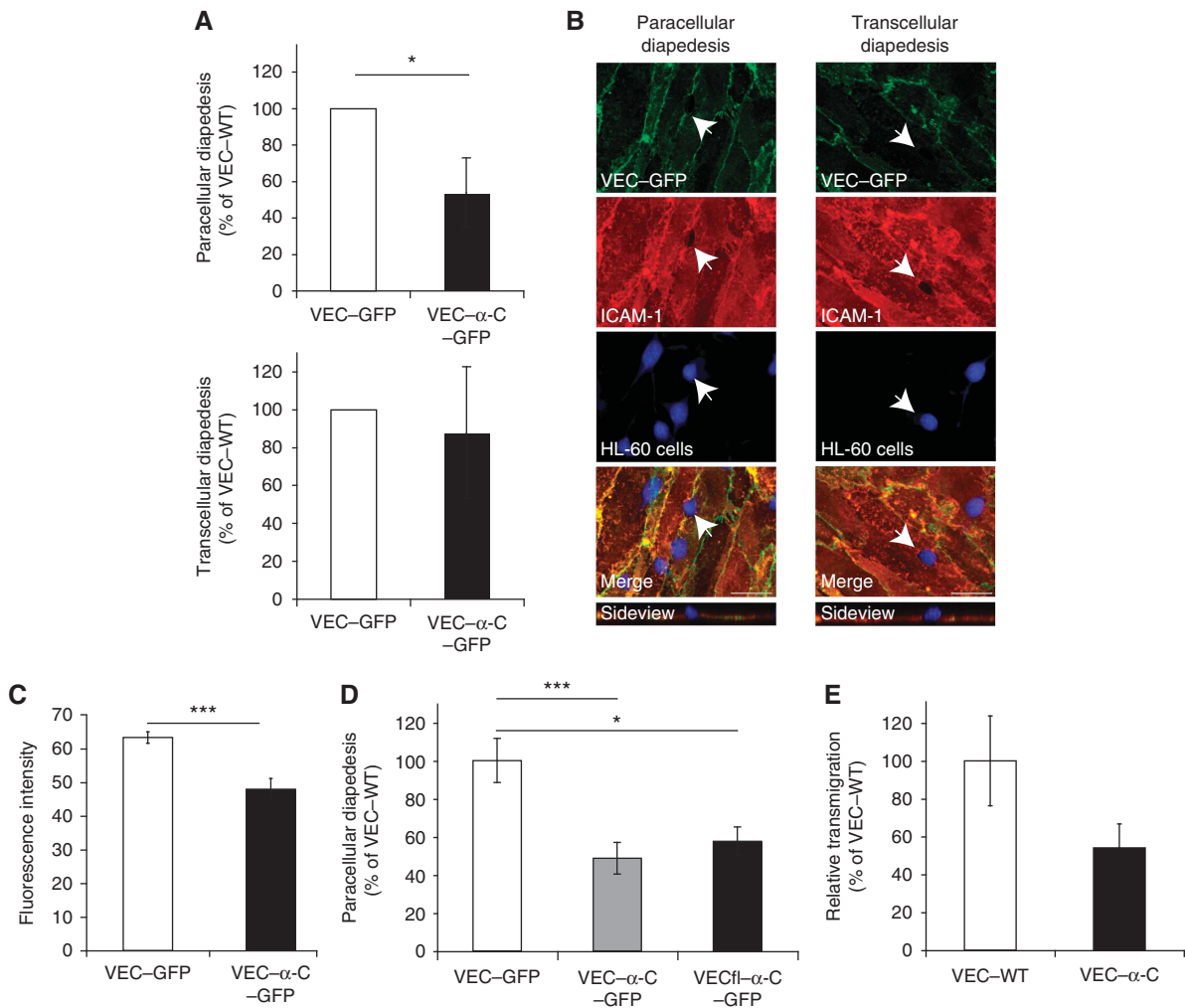
Figure 5 VE-cadherin–α-catenin strongly reduces paracellular, but not transcellular diapedesis. (**A**) VEC–GFP or VEC–α-C–GFP was expressed by adenoviral vectors in HUVEC and paracellular and transcellular diapedesis were analysed as described in Materials and methods. DMSO differentiated granulocytic-HL60 cells were incubated with adenovirus transduced, TNF-α activated HUVEC for 20 min followed by fixation, staining and scoring of paracellular (top) and transcellular (bottom) diapedesis. In each case, the number of neutrophils migrating across VEC–GFP infected cells was set to 100%. A total of 39 or 44 areas containing 1090 or 1042 HL60 cells (including all loosely attached, adhering, transmigrating and transmigrated cells) were analysed for VEC–GFP and VEC–α-C–GFP expressing HUVEC, respectively. In all, 14% of these HL60 cells were transmigrating through VEC–GFP expressing HUVEC of which 96% migrated paracellular and 4% transcellular. (**B**) Representative immunofluorescence images of granulocytic-HL60 cells migrating through the transcellular or the paracellular route, endothelial cell contacts stained for VEC–GFP (green), HL60 stained by Cell Tracker (blue), apical endothelial cell surface stained for ICAM-1 (red). Projections of z-stacks taken on an LSM Zeiss 510 Meta, bars = 20 μm. (**C**) Quantification of the expression levels of VEC–GFP and VEC–α-C–GFP by determining fluorescence intensity in 75 randomly selected ROIs of 50 μm^2 at sites of cell contacts in HUVEC used for transmigration assays. (**D**) Transduced, TNF-α activated HUVEC cells expressing VEC–GFP, VEC–α-C–GFP or VECfl–α-C–GFP were incubated with granulocytic-HL60 cells for 20 min followed by fixation and staining. Paracellular migration through VEC–GFP expressing cells was set to 100%. A total of 18, 20 and 11 stacks containing 421, 426 and 302 HL60 cells with 74, 40 and 26 paracellular migrating cells were counted for VEC–GFP, VEC–α-C–GFP and VECfl–α-C–GFP expressing HUVEC, respectively. (**E**) Mouse PMNs were allowed to transmigrate for 30 min through TNF-α-stimulated endothelioma cells from VEC–WT and VEC–α-C mice grown on 3 μm pore size transwell filters. Transmigration through VEC–WT cells was set to 100%. *$P \leqslant 0.05$, ***$P \leqslant 0.001$; (**A, D**) Mann Rank Sum Test, (**C, E**) *t*-test.

VEC–α-C were co-precipitated with p120 from lung lysates of VEC–WT and VEC–α-C mice (Figure 8D). Furthermore, VE-cadherin–GFP or VE-cadherin–α-catenin–GFP expressed in HUVEC cells were endocytosed with similar efficiency. Uptake was determined after 15, 30 and 60 min by staining of endocytosed anti-VE-cadherin antibody (Figure 8E and F).

Reduced detergent extractability and membrane mobility of VE-cadherin–α-catenin

To elucidate how the covalent fusion of VE-cadherin with α-catenin enhances the stability of endothelial cell contacts,

we tested whether the interaction of VE-cadherin with the cytoskeleton would be altered. We used endothelioma cells for this analysis, which we had generated from VEC–WT and VEC–α-C mice. Western blot analysis of the detergent soluble and insoluble fraction of VE-cadherin and VEC–α-C in these cell lines revealed that 30% of wild-type VE-cadherin, but 60% of VEC–α-C were resistant to detergent extraction (Figure 9A). These results suggest that VEC–α-C attaches to the actin cytoskeleton more strongly than VE-cadherin.

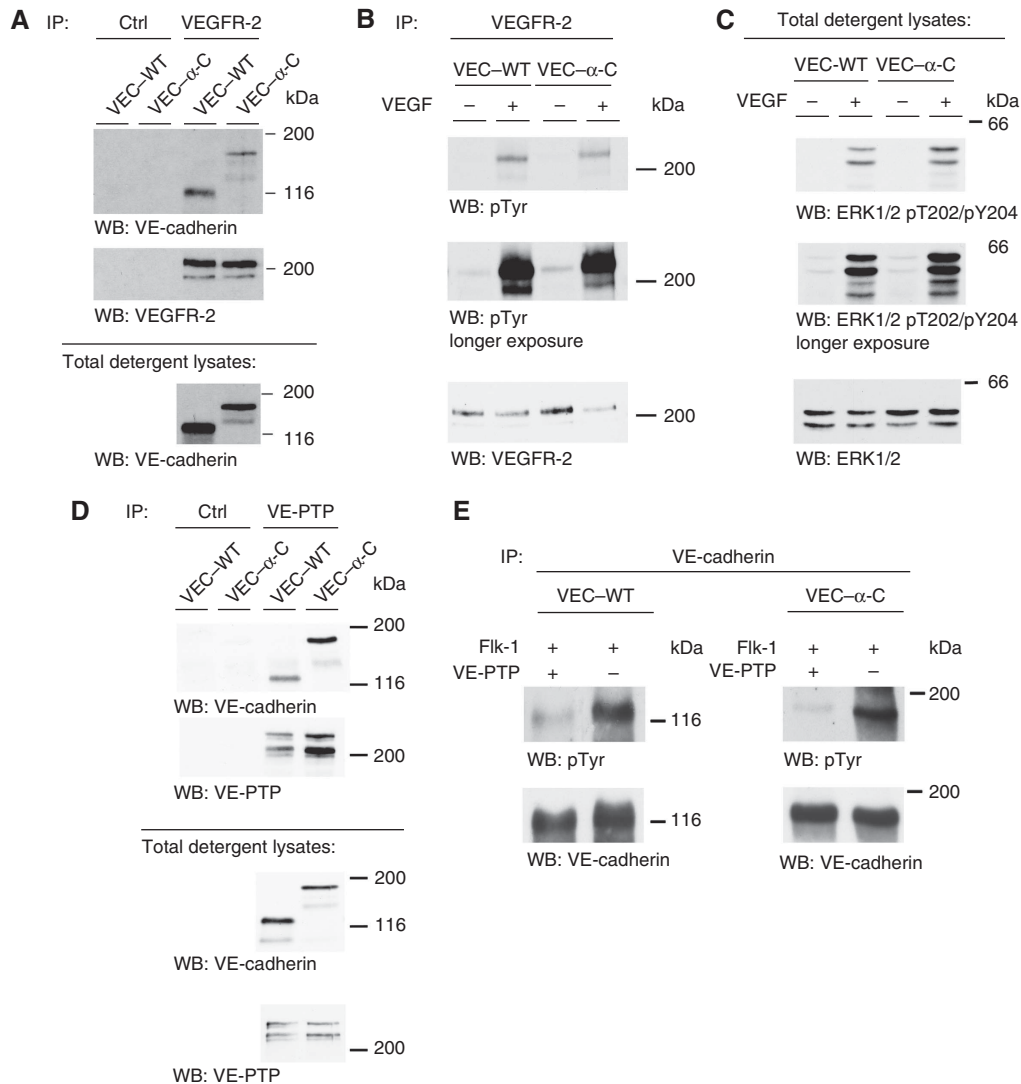We verified this by comparing the membrane mobility of VEC–α-C and VE-cadherin using fluorescence recovery after

Figure 6 VEGFR-2 signalling and VE-cadherin/VE-PTP interactions are not affected by fusion of VE-cadherin with α-catenin. (**A**) Cell lysates of confluent endothelioma cells generated from VEC–WT or VEC–α-C mice were immunoprecipitated (IP) with control antibodies (Ctrl) or antibodies against VEGFR-2 and precipitates were analysed by western blotting (WB) with antibodies to VE-cadherin and VEGFR-2, documenting association of VEGFR-2 with VE-cadherin and VEC–α-C. Note: Total detergent lysates contained less solubilized VEC–α-C than VE-cadherin protein (see below). (**B, C**) Confluent VEC–WT and VEC–α-C endothelioma cells were stimulated with VEGF (100 ng/ml) for 5 min, followed by (**B**) immunoblotting of immunoprecipitated VEGFR-2 with antibodies against phosphotyrosine (pTyr) and VEGFR-2; and (**C**) against phospho-Erk1/2 (pT202/pY204) and Erk1/2. Molecular weight markers are indicated on the right. (**D**) Anti-VE-PTP and control (Ctrl) immunoprecipitates from VEC–WT and VEC–α-C endothelioma cells (top panel) or total cell lysates (bottom panel) were immunoblotted for VE-cadherin or for VE-PTP (as indicated). (**E**) COS cells were transfected with VEC–WT (left) or VEC–α-C (right) and co-transfected with Flk1 and with (+) or without (−) VE-PTP. VE-cadherin immunoprecipitates were immunoblotted for phosphotyrosine (pTyr) or for VE-cadherin. Figure source data can be found with the Supplementary Information.

photobleaching (FRAP). To this end, the two proteins fused with GFP were expressed in HUVEC using adenoviral vectors. As shown in Figure 9C and D, FRAP was clearly delayed for VEC–α-C–GFP when compared with VEC–GFP. Quantification revealed a significantly increased halftime of recovery for VEC–α-C–GFP (Figure 9F). Furthermore, a much larger faction of VEC–α-C–GFP molecules was immobile than of VEC–GFP molecules (Figure 9E). To test whether the mobility of the two versions of VE-cadherin was indeed dependent on the actin cytoskeleton, we performed this analysis with cells that had been treated with latrunculin, to impair the formation of cortical actin. This increased the mobility of both VEC–α-C and VE-cadherin and enlarged the mobile fraction of both proteins (Figure 9E and F). In line

with these results, expression of VEC–α-C–GFP straightened endothelial cell contacts (Figure 9B), a clear sign for the enhancement of cell contact integrity. Collectively, these results indicate that VEC–α-C associates more efficiently with the actin cytoskeleton than VE-cadherin, suggesting that this is the reason for the stabilization of endothelial cell contacts.

Discussion

In this study, we have investigated whether leukocytes require opening of endothelial cell contacts in order to leave blood vessels and enter into tissues. To answer this, we wanted to strengthen the stability of endothelial junctions
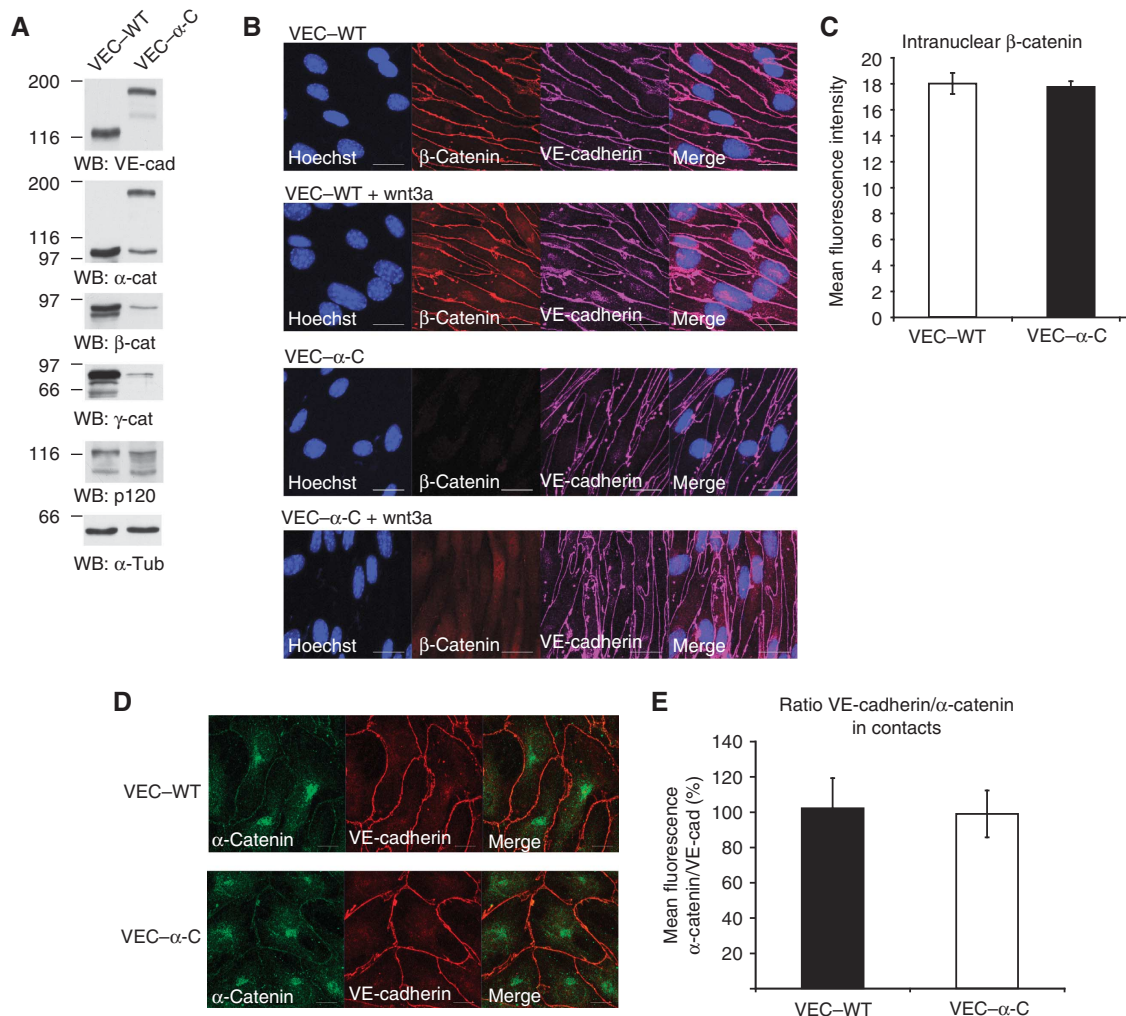
Figure 7 Catenin expression and subcellular distribution in VEC–WT and VEC–α-C cells. (**A**) Triton lysates of endothelioma cells established from VEC–WT and VEC–α-C mice were immunoblotted for VE-cadherin, α-catenin, β-cat, plakoglobin, p120 and α-tubulin (as indicated). (**B**) VEC–WT and VEC–α-C endothelioma cells were treated for 14 h with or without wnt3a, fixed, permeabilized and stained for nuclei, VE-cadherin and β-catenin. (**C**) Quantification of nuclear β-catenin staining after wnt3a stimulation, *t*-test. (**D**) Immunofluorescence staining of VEC–WT and VEC–α-C endothelioma cells for VE-cadherin and α-catenin. (**E**) Quantification of the ratio of VE-cadherin/α-catenin staining at cell contact as shown in (**D**), *t*-test. Figure source data can be found with the Supplementary Information.

in gene-targeted mice by irreversibly fusing VE-cadherin with α-catenin. This modification of VE-cadherin indeed blocked the induction of vascular permeability by two different, very potent inflammatory stimuli in the skin, demonstrating, first that VEC–α-C strongly stabilizes endothelial junctions *in vivo*, and second that induction of vascular permeability requires the opening of gaps between endothelial cells. Leukocyte extravasation was strongly reduced in cremaster, lung and skin of VEC–α-C mice stimulated by various inflammatory mediators, indicating that most extravasating leukocytes require the opening of endothelial junctions to enter these tissues. Finally, our results demonstrate that the VE-cadherin–catenin complex is in several tissues an essential target for the opening of endothelial junctions and for leukocyte extravasation. Since the fusion between VE-cadherin and α-catenin inhibits both processes *in vivo* and strongly enhances the interaction of VE-cadherin with the actin cytoskeleton, we conclude that the plasticity of this complex allows destabilization of its interaction with the actin cytoskeleton, which in

turn is required for the induction of vascular permeability and leukocyte extravasation.

The question which route leukocytes take to migrate through endothelial cell barriers has been analysed since the 60s in numerous studies and various species by electron microscopy. Several studies suggested that leukocytes exclusively use either the paracellular or the transcellular pathway but had not been based on serial section analysis, and therefore were inconclusive. Only a few, very thorough studies analysed serial sections, but again provided contradictory results that either argued exclusively for the paracellular diapedesis route (Marchesi, 1961; Schoefl, 1972; Anderson and Anderson, 1976), or for the transcellular route (Marchesi and Gowans, 1964; Farr and DeBruyn, 1975; Feng *et al*, 1998; Hoshi and Ushiki, 1999) . Due to the tedious procedure of serial section analysis, only few leukocytes could be analysed in each of these studies. In contrast, our approach of selectively inhibiting the paracellular route allows a quantitative analysis of whole tissue areas and allows the comparison of
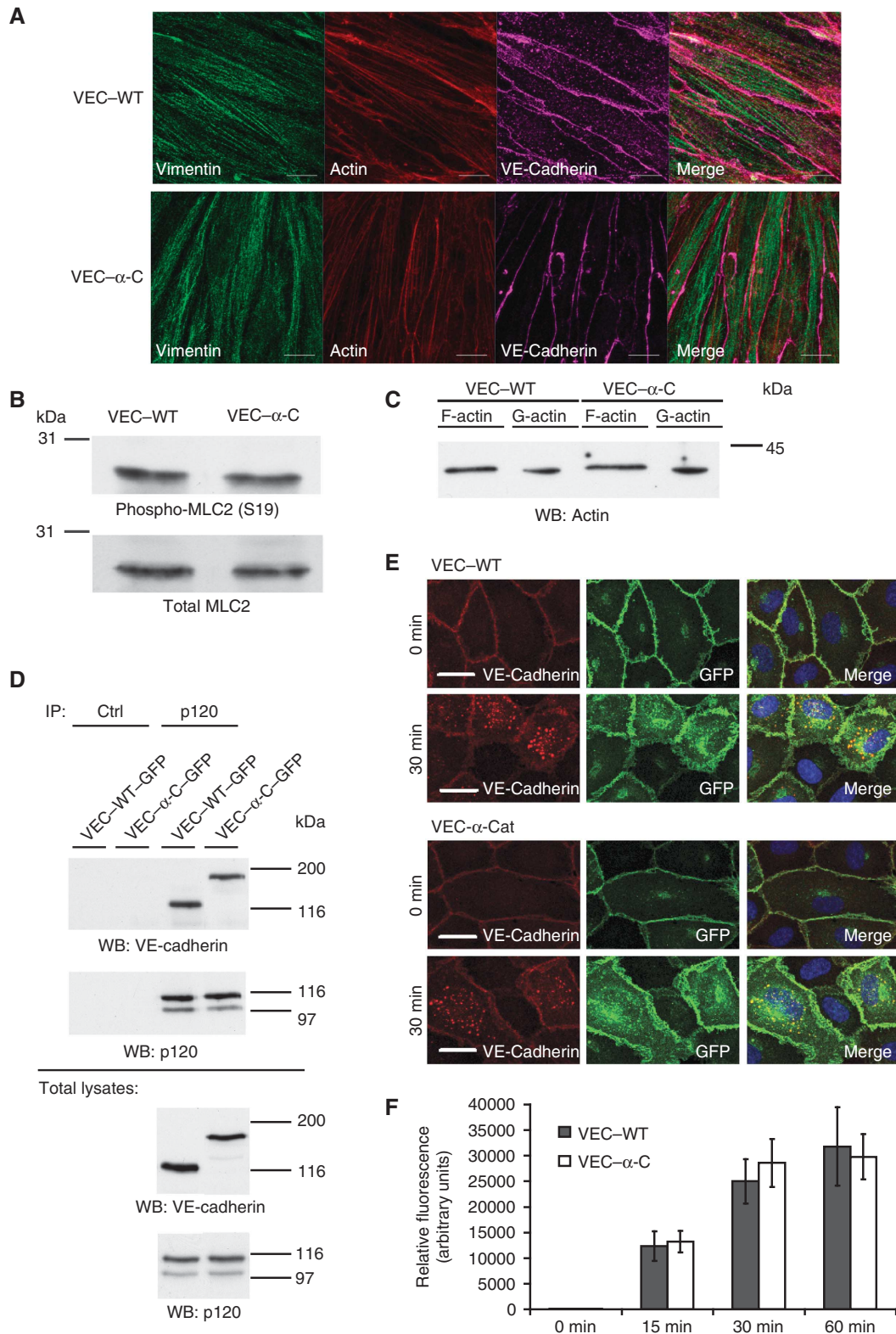
Figure 8 Cytoskeletal organization and VE-cadherin endocytosis are not affected by VEC–α-C. (**A**) Immunofluorescence staining of VEC–WT and VEC–α-C endothelioma cells for vimentin, VE-cadherin and actin (as indicated). (**B**) Western blots of cell lysates of the same cells for total myosin light chain (MLC2) and its phosphorylated form. (**C**) F-actin and G-actin were isolated from the same cells and detected by immunoblotting. (**D**) Lung lysates of VEC–WT and VEC–α-C mice were immunoprecipitated for p120 or with control antibodies (Ctrl) and precipitates were immunoblotted for p120 or VE-cadherin. Bottom: respective immunoblots of total lung lysate aliquots. (**E, F**) Endocytosis of VE-cadherin. (**E**) VE-cadherin–GFP (VEC–WT) or VE-cadherin–α-catenin–GFP (VEC–α-C) was expressed by adenoviral vectors in HUVEC cells, incubated with an anti-VE-cadherin antibody at 4°C, and after washing away excess of antibody, cells were allowed to endocytose VE-cadherin for 0 or 30 min. Cells were fixed, permeabilized and stained with a secondary antibody against the first antibody (red). GFP is seen in green, merge to the right. (**F**) Quantification of intracellular (red) VE-cadherin staining of HUVEC that had endocytosed VE-cadherin–GFP (VEC–WT) or VE-cadherin–α-catenin–GFP (VEC–α-C) for 0, 15, 30 or 60 min, *t*-test. Figure source data can be found with the Supplementary Information.
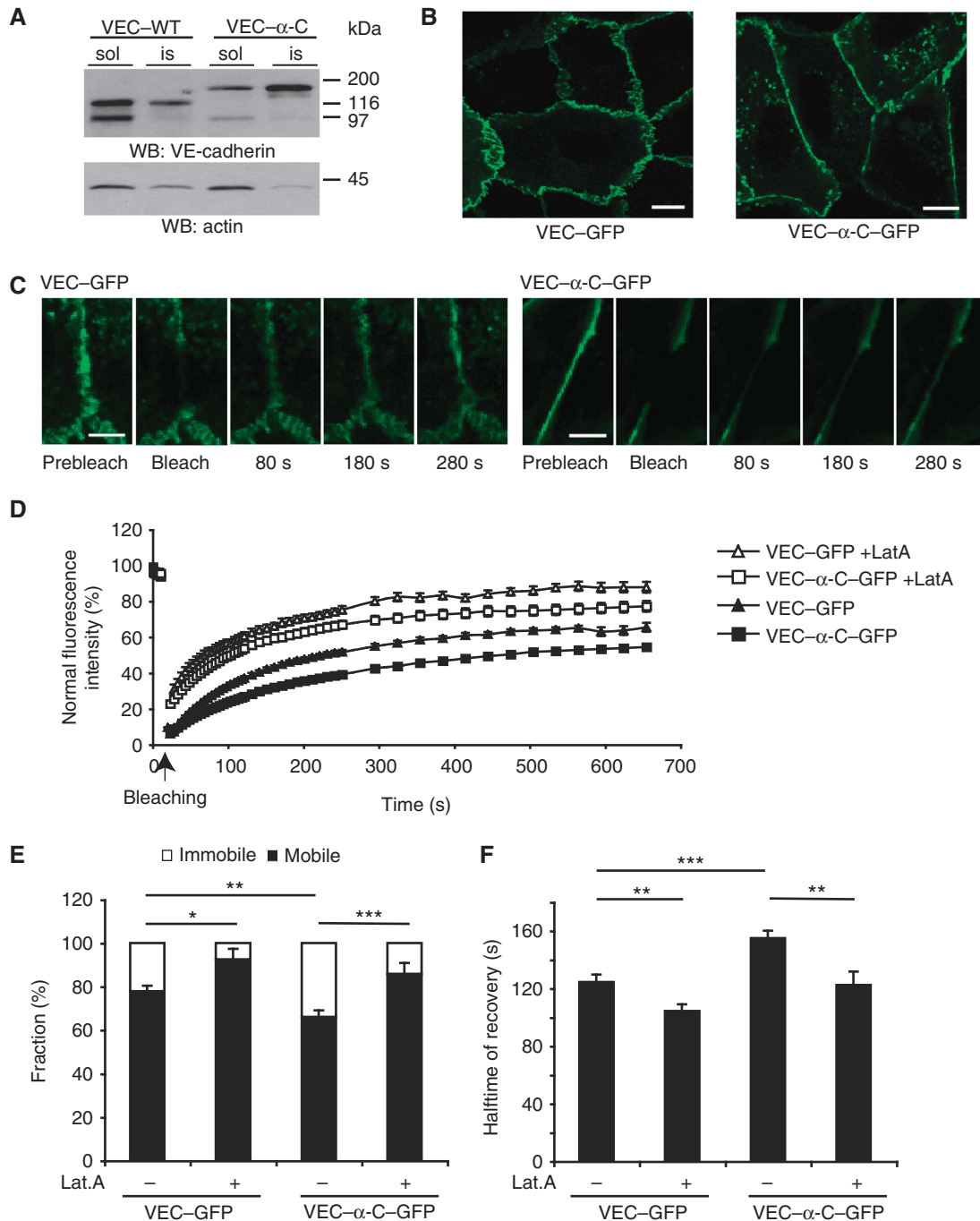
Figure 9 Fusion of VE-cadherin with α-catenin decreases detergent extractability and membrane mobility. (**A**) Embryonic endothelioma cell lines established from mutant VEC–WT and VEC–α-C embryos were extracted with 1% NP-40 followed by immunoblot analysis of soluble (sol) and insoluble (is) fractions as described in Materials and methods. Molecular weight markers are indicated on the right. (**B**) Representative images of HUVEC expressing VEC–GFP or VEC–α-C–GFP used for FRAP analysis. Note the straightened cell contacts in cells expressing VEC–α-C–GFP compared with VEC–GFP. Bars = 10 μm. (**C**) Representative images of cell contact areas of HUVEC expressing VEC–GFP or VEC–α-C–GFP at indicated time points prior and post photobleaching. Bars = 5 μm. (**D**) Time course of fluorescence recovery at bleached areas of cell contacts of vehicle-treated HUVEC expressing VEC–GFP (black triangles, 24 areas analysed) or VEC–α-C–GFP (black boxes, 32 areas analysed) and the respective latrunculin A treated, transduced HUVEC (+ LatA, open triangles or boxes, 19 and 14 areas analysed). (**E, F**) Mobile (white) and immobile (black) fraction (**E**) and recovery halftime of VEC–GFP or VEC–α-C–GFP (**F**) in transduced HUVEC treated with vehicle or latrunculin A (as indicated) calculated from the curves shown in (**D**). $*P \leqslant 0.05$; $**P \leqslant 0.01$; $***P \leqslant 0.001$, t-test. Figure source data can be found with the Supplementary Information.

various tissues and inflammatory conditions within one study. VEC–α-C is ideally suited to block selectively the paracellular and not the transcellular diapedesis pathway, as VE-cadherin is specifically expressed at endothelial junctions and represents the major denominator of endothelial cell contact stability. In agreement with this, our *in vitro*

transmigration experiments provided direct evidence that VEC–α-C indeed selectively inhibited the paracellular and not the transcellular diapedesis route.

Inhibition of leukocyte extravasation by VEC–α-C was strong suggesting that the majority of neutrophils entering into the cremaster and the lung and more than half of the

activated lymphocytes recruited to inflamed skin extravasate through endothelial junctions. A limitation of our approach is that we cannot distinguish whether the residual leukocyte extravasation in VEC–α-C mice is due to the fact that the extravasating leukocytes were still able to open endothelial junctions, although with reduced efficiency, or whether this residual leukocyte extravasation is due to an alternative transcellular pathway. In this respect, it is important to note that even *in vitro* the expression of VEC–α-C in HUVEC only inhibited neutrophil diapedesis by about 50%, although the paracellular route was clearly the major pathway. Even in endothelioma cells established from VEC–α-C mice inhibition was limited to about 50%. This indicates that VEC–α-C may not completely and under any circumstances lock endothelial junctions. Thus, the inhibitory effects we have observed allow a minimum estimation of the extent, to which the paracellular route is used by extravasating leukocytes.

We were surprised to see that lymphocyte homing was not at all affected in VEC–α-C mice. One possible explanation is that naive lymphocytes may extravasate through a transcellular route in HEV of lymph nodes. Alternatively, it is possible that endothelial cells in HEV might be endued with additional molecular mechanisms that enable them to open their junctions despite of expressing VEC–α-C. A third possibility would be that lymphocyte diapedesis in venules of these tissues is so efficient that once a lymphocyte has managed to open an endothelial junction it is immediately followed by another lymphocyte through the same junctional gap before it closes again, resulting in one diapedesing lymphocyte still present in an inter-endothelial gap, while the next one already enters this gap. Such situations have actually been described for HEV in lymph nodes.

Similarly to the two routes of leukocyte extravasation, two different mechanisms for the induction of vascular permeability have been suggested. Alksne (1959) reported that histamine stimulates the transcellular exit of carbon particles through endothelial cells, and this mechanism was confirmed and extended to various vessel structures and stimuli (Feng *et al*, 2002). In contrast, Majno and Palade (1961) showed that histamine-induced exudation occurred via gap formation between endothelial cells. This is in perfect agreement with the excellent work by Baluk and McDonald (Baluk *et al*, 1997, 1998), who showed by transmission and scanning electron microscopy and light microscopy of silver nitrate-labelled endothelial contacts *in vivo* that allergens and other stimuli induced the formation of gaps between cells but no transcellular holes. These studies illustrate that despite the excellent electron microscopy performed by various laboratories, even the direct morphological analysis provides diverging results on the nature of the pathway that enables induction of vascular permeability. In this respect, it is remarkable that the VEC–α-C mice were indeed resistant to potent permeability-inducing agents such as histamine and VEGF. Thus, our approach of selectively blocking the paracellular pathway enabled us to study the mechanism of permeability induction independent of a morphological technique. In addition, VEC–α-C mice allow robust quantification of vascular permeability for a large tissue area, which extends electron microscopic studies, where the observation is limited to the analysis of a few vessels. We conclude that both VEGF and histamine, stimuli that act via completely different receptor pathways, exclusively induce vascular permeability by destabilizing endothelial cell contacts.

It has been shown that antibodies against VE-cadherin can enhance leukocyte extravasation (Gotsch *et al*, 1997). However, this merely established that artificial opening of endothelial cell contacts by antibodies creates a situation of which leukocytes can take advantage. In other words, destabilizing VE-cadherin interactions is sufficient to facilitate leukocyte extravasation, yet whether it is indeed necessary *in vivo* has never been analysed. Transmigration assays using cultured endothelial cells transfected with certain tyrosine/phenylalanine replacement mutants of VE-cadherin suggested that VE-cadherin represents an essential target during the leukocyte diapedesis mechanism *in vitro* (Allingham *et al*, 2007; Turowski *et al*, 2008). However, this was based on overexpression of the mutant forms of VE-cadherin, was limited to *in vitro* studies and except for one tyrosine mutant, there is no agreement on whether other mutants were inhibitory or not. Our results demonstrate for the first time *in vivo* that VE-cadherin represents an essential barrier for extravasating leukocytes in several tissues, which needs to be opened during diapedesis.

Since lack of VE-cadherin has been shown to affect cellular functions such as VEGR-2 signalling (Lampugnani *et al*, 2006) and expression of claudin 5 (Taddei *et al*, 2008), we tested whether replacing VE-cadherin by VEC–α-C would cause any such side effects. We found that VEGFR-2 signalling was normal and unaffected in endothelial cells isolated from our gene-targeted mice. Likewise, expression of claudin 5 was normal. We could also exclude that lack of the β-catenin-binding C-terminal 75 amino acids of VE-cadherin in our VEC–α-C fusion protein would be responsible for the inhibitory effect on leukocyte diapedesis, as a similar construct containing full-length VE-cadherin had the same inhibitory effect. Deletion of the β-catenin binding site of VE-cadherin has been shown to cause lethality at E9.5 due to impaired protection against apoptosis and a lack of VEGFR-2 signalling (Carmeliet *et al*, 1999). Interestingly, this defect was rescued in our VEC–α-C mice by the fusion with α-catenin, as up to E13.5 VEC-α-C homozygous embryos appeared at Mendelian frequencies (data not shown). In addition, we could exclude that VE-PTP association with VE-cadherin, wnt/β-catenin signalling or cytoskeletal organization and cortical actin formation would be altered by VEC–α-C. Collectively, besides it's clear stabilizing effect on endothelial cell contacts, we have presently no indication that VEC–α-C influences signalling events differently than WT VE-cadherin.

Our findings with the VEC–α-C mice raise the question, how VE-cadherin–α-catenin stabilizes endothelial cell contacts? It has been well documented that cadherins require the link to α-catenin via β/γ-catenin to support optimal adhesion and cell contact integrity (Ozawa *et al*, 1989; Hirano *et al*, 1992; Navarro *et al*, 1995). In contrast to this model, it was recently shown that α-catenin only binds directly to the actin cytoskeleton if it is not associated with the cadherin–β-catenin complex (Yamada *et al*, 2005). Whether the fusion of α-catenin with VE-cadherin allows or does not allow direct binding to actin is not known. However, independent of the question whether α-catenin links cadherins to the actin cytoskeleton by direct interactions, there is good evidence for a potentially indirect association between the cadherin–

catenin complex and the actin cytoskeleton (Abe and Takeichi, 2008; Noda *et al*, 2010; Yonemura *et al*, 2010). One possibility to weaken cadherin-mediated adhesion would be to dissociate the cadherin–catenin complex, which in turn would destabilize the indirect link of VE-cadherin to the actin cytoskeleton. Indeed, it was recently shown that VEGF can induce the dissociation of β-catenin from VE-cadherin (Monaghan-Benson and Burridge, 2009) and it is possible that this may be involved in the opening of endothelial cell contacts. Our results clearly demonstrate that the covalent fusion of α-catenin with VE-cadherin stabilizes endothelial cell contacts and at the same time intensifies the interaction of VE-cadherin with the actin cytoskeleton, as we documented by reduced detergent extractability, reduced membrane mobility of VE-cadherin–α-catenin and the dependence of this mobility on the polymerization status of the actin cytoskeleton. Our results on membrane mobility are in good agreement with recent results on a different VE-cadherin–α-catenin fusion protein expressed in HUVEC (Noda *et al*, 2010). Collectively, our results suggest that the plasticity of the VE-cadherin–catenin complex and the regulation of the link with the actin cytoskeleton is a central step in opening the junctional pathway during leukocyte extravasation and induction of vascular permeability.

In summary, we have shown that induction of vascular permeability by various inflammatory stimuli as well as leukocyte extravasation in various inflamed tissues such as cremaster, lung and skin relies on the junctional pathway between endothelial cells. In these tissues, the VE-cadherin–catenin complex and its interaction with the actin cytoskeleton represent an essential molecular target that is addressed in both processes to overcome the endothelial barrier of the vessel wall.

Materials and methods

Blood vessel permeability assay
A modified Miles assay for the induction of vascular permeability in the skin was performed as described previously (Wegmann *et al*, 2006) using three to five 8–12-week-old sex-matched VEC–WT or VEC–α-C mice. Skin areas were excised 30 min after stimulation with 100 ng VEGF$_{164}$ or 225 ng histamine.

Delayed type hypersensitivity
Immigration of radioactively [^{51}Cr]-labelled T cells into inflamed skin was analysed with the DTH model as described previously (Bixel *et al*, 2004) Briefly, T cells had been isolated from lymph nodes of DNFB-treated mice, radioactively labelled and injected into at least four 7–12-week-old sex-matched VEC–WT or VEC–α-C recipient mice whose skin had been sensitized and challenged with DNFB. Immigration of T cells was analysed 5 h after adoptive transfer of radioactively labelled T cells from sensitized VEC–WT mice into VEC–WT or VEC–α-C recipient mice.

Neutrophil recruitment into the lung
Neutrophil recruitment into the lung was analysed in a murine model of LPS-induced pulmonary inflammation as previously described (Zarbock *et al*, 2008). Four hours after induction of pulmonary inflammation by exposing mice to aerosolized LPS, the number of neutrophils in the bronchoalveolar lavage (BAL) was determined.

Intravital microscopy
VEC–WT or VEC–α-C mice received an intrascrotal injection of 50 ng IL-1β in 0.3 ml saline. Four hours later, mice were anaesthetised with an intraperitoneal injection of ketamine hydrochloride (125 mg/kg), atropine sulphate (0.025 mg/kg) and xylazine

(12.5 mg/kg) and the mouse cremaster muscle was used to study neutrophil recruitment as previously described (Petri *et al*, 2010).

Lymphocyte homing
The migration of naive T cells into lymph nodes was analysed using a lymph node homing assay with radioactively [^{51}Cr]-labelled T cells as described (Hamann and Jonas, 1997). Briefly, naive lymphocytes were isolated from PLN and MLN from VEC–WT mice and purified by gradient centrifugation on top of 5 ml Lympholyte-M solution. An aliquot of cells was stained with an antibody against CD3 and analysed by flow cytometry. T cells were labelled with 40 μCi/ml sodium [^{51}Cr] chromate for 1 h at 37°C, and 2×10^6 cells were injected in 200 μl PBS into the tail vein of each mouse. After 3 h, mice were sacrificed and the radioactivity in PLN and MLN as well as the remainder of the mice was measured. The γ-radiation was converted into counts per minute (cpm) and the percentage radiation of each organ compared with the whole organism was calculated using the following formula: cpm % organ = cpm organ/cpm total × 100%.

Analysis of neutrophil transmigration in cremasteric venules using confocal immunofluorescence microscopy
Transmigration of neutrophils using confocal immunofluorescence microscopy was performed as described previously (Bixel *et al*, 2010). Three VEC–WT or VEC–α-C mice were used for each assay and the number of neutrophils was analysed 3 h after intrascrotal injection of 50 ng IL-1β in 0.3 ml saline. Whole-mount immunostainings were performed using PECAM-1 antibodies and antibodies against MRP-14. Neutrophils were classified into two groups: Group A representing neutrophils present in the vessel lumen or at the level of endothelium, group B comprising all neutrophils that have already extravasated, including those with still part of their body between endothelial cells and those located between endothelium and basement membrane.

Analysis of transcellular and paracellular diapedesis in vitro
HUVEC were plated at confluency on fibronectin-coated glass slides and cultured for 24 h. Then, cells were infected with VEC–GFP, VEC–α-C–GFP or VECfl–α-C–GFP adenovirus with an MOI of 3, cultured for 24 h and subsequently stimulated for 16 h with TNF-α (50 ng/ml). HL60 cells were differentiated with 1.3% DMSO for 3 days. They were then stained with 15 μM CellTracker Blue (Invitrogen) according to the manufacturer's instructions, added to the HUVEC monolayer and allowed to transmigrate for 20 min at 37°C. Excess HL60 cells were decanted, but not washed away and samples were fixed using 4% PFA for 5 min at 37°C, permeabilized using 0.5% Triton X-100 and stained for ICAM-1. Primary antibodies were detected with Alexa Fluor-568-coupled secondary antibodies. The route of leukocyte diapedesis was determined as described previously (Corada *et al*, 1999) from the relative distribution of CellTracker Blue, ICAM-1 and VE-Cadherin–GFP. *In vitro* transmigration assays with endothelioma cells were performed as described previously (Nottebaum *et al*, 2008) using transwell filters with a pore size of 3 μm (Corning Inc.).

Fluorescence recovery after photobleaching
In all, 24 h after plating HUVEC at confluence on 8-well μ dishes (Ibidi), cells were infected with VEC–GFP or VEC–α-C–GFP adenovirus with an MOI of 90. The cells were then cultured for another 20 h and starved in medium 199 with 1% BSA for 2 h. Live cell imaging of GFP-positive cells was performed using an Inverse SP5 laser-scanning confocal microscope (Leica) with a ×63 objective lens at 37°C with 5% CO$_2$ using a heating chamber (Leica). GFP fluorescence at the cell–cell contacts was bleached for 10 s using a 488-nm Argon laser at maximum power. Images were acquired and fluorescence intensities analysed using the LAS AF Lite version 2.2.0 software (Leica). Prior to bleaching, five images were acquired, after bleaching a time series mode for post bleaching image acquisition was set for 20 acquisitions every 5 s, then 15 acquisitions every 10 s and subsequently 15 acquisitions every 30 s. Using Excel software, the values of fluorescence intensities post bleach were normalized with the fluorescence intensity prior to the

bleach and were corrected for the overall loss in fluorescence intensity due to image scanning. Latrunculin A (0.2 µg/ml) was applied to cells for 5 min after starving cells for 2 h in medium 199 with 1% BSA before starting the FRAP experiment.

Systemic leukocyte blood counts

The number of white blood cells was determined using a cell counter (CASY TT +, Schärfe System). Differential leukocyte counts were determined after staining leukocytes for Gr-1, CD4 and CD8 followed by flow cytometry.

Immunofluorescence and whole-mount stainings

Whole-mount staining of cremaster muscle tissue and omental tissues was performed as described previously (Bixel *et al*, 2010). For immunofluorescence stainings of cell monolayers, cells were fixed with 2% PFA, permeabilized with 0.5% Triton X-100 and blocked in 3% BSA. Antibody stainings were performed in 1% BSA + 0.1% Triton X-100. For staining of vimentin and actin, cells were fixed in ethanol at −20°C for 20 min.

Microscopy

Z-stack images were acquired using a confocal laser-scan microscope (LSM 510 META; Carl Zeiss, Inc.) with 20 × /NA 0.8, 40 × / NA 1.2 or 63 × /NA 1.4 objectives (Carl Zeiss, Inc.) and were analysed using the LSM Image Examiner 3D software (Carl Zeiss). Mean fluorescence intensities were calculated using ImageJ software.

Statistical analysis

Data sets were checked for normality (Shapiro–Wilk) and equal variance. *P*-values were determined by Student's *t*-test if allowed or otherwise by Mann–Whitney Rank Sum Test. Analysis was performed using SigmaPlot 10.0. Values are presented as means ± standard error of mean (s.e.m.). *$P < 0.05$; **$P < 0.01$; ***$P < 0.001$.

All animal experiments were performed in accordance with the local animal protection legislation (Bezirksregierung Muenster).

Conflict of interest

The authors declare that they have no conflict of interest.

References

Abe K, Takeichi M (2008) EPLIN mediates linkage of the cadherin catenin complex to F-actin and stabilizes the circumferential actin belt. *Proc Natl Acad Sci USA* **105**: 13–19

Alksne JF (1959) The passage of colloidal particles across the dermal capillary wall under the influence of histamine. *Q J Exp Physiol Cogn Med Sci* **44**: 51–66

Allingham MJ, van Buul JD, Burridge K (2007) ICAM-1-mediated, Src- and Pyk2-dependent vascular endothelial cadherin tyrosine phosphorylation is required for leukocyte transendothelial migration. *J Immunol* **179**: 4053–4064

Anderson AO, Anderson ND (1976) Lymphocyte emigration from high endothelial venules in rat lymph nodes. *Immunology* **31**: 731–748

Baluk P, Bolton P, Hirata A, Thurston G, McDonald DM (1998) Endothelial gaps and adherent leukocytes in allergen-induced early- and late-phase plasma leakage in rat airways. *Am J Pathol* **152**: 1463–1476

Baluk P, Hirata A, Thurston G, Fujiwara T, Neal CR, Michel CC, McDonald DM (1997) Endothelial gaps: time course of formation and closure in inflamed venules of rats. *Am J Physiol* **272**: L155–L170

Bixel G, Kloep S, Butz S, Petri B, Engelhardt B, Vestweber D (2004) Mouse CD99 participates in T cell recruitment into inflamed skin. *Blood* **104**: 3205–3213

Bixel MG, Li H, Petri B, Khandoga AG, Khandoga A, Zarbock A, Wolburg-Buchholz K, Wolburg H, Sorokin L, Zeuschner D, Maerz S, Butz S, Krombach F, Vestweber D (2010) CD99 and CD99L2 act at the same site as, but independently of, PECAM-1 during leukocyte diapedesis. *Blood* **116**: 1172–1184

Carman CV, Sage PT, Sciuto TE, de la Fuente MA, Geha RS, Ochs HD, Dvorak HF, Dvorak AM, Springer TA (2007) Transcellular diapedesis is initiated by invasive podosomes. *Immunity* **26**: 784–797

Carman CV, Springer TA (2004) A transmigratory cup in leukocyte diapedesis both through individual vascular endothelial cells and between them. *J Cell Biol* **167**: 377–388

Carmeliet P, Lampugnani M-G, Moons L, Breviario F, Compernolle V, Bono F, Balconi G, Spagnuolo R, Oosthuyse B, Dewerchin M, Zanetti A, Angellilo A, Mattot V, Nuyens D, Lutgens E, Clotman F, de Ruiter MC, Gittenberger-de Groot A, Poelmann R, Lupu F *et al* (1999) Targeted deficiency or cytosolic truncation of the VE-cadherin gene in mice impairs VEGF-mediated endothelial survival and angiogenesis. *Cell* **98**: 147–157

Corada M, Mariotti M, Thurston G, Smith K, Kunkel R, Brockhaus M, Lampugnani MG, Martin-Padura I, Stoppacciaro A, Ruco L, McDonald DM, Ward PA, Dejana E (1999) Vascular endothelial-cadherin is an important determinant of microvascular integrity *in vivo*. *Proc Natl Acad Sci USA* **96**: 9815–9820

Farr AG, DeBruyn PPH (1975) The mode of lymphocyte migration through postcapillary venule endothelium in lymph node. *Am J Anat* **143**: 55–92

Feng D, Nagy JA, Dvorak HF, Dvorak AM (2002) Ultrastructural studies define soluble macromolecular, particulate, and cellular transendothelial cell pathways in venules, lymphatic vessels, and tumor-associated microvessels in man and animals. *Microsc Res Tech* **57**: 289–326

Feng D, Nagy JA, Pyne K, Dvorak HF, Dvorak AM (1998) Neutrophils emigrate from venules by a transendothelial cell pathway in response to FMLP. *J Exp Med* **187**: 903–915

Gotsch U, Borges E, Bosse R, Böggemeyer E, Simon M, Mossmann H, Vestweber D (1997) VE-cadherin antibody accelerates neutrophil recruitment *in vivo*. *J Cell Sci* **110**: 583–588

Hamann A, Jonas P (1997) *Lymphocyte Migration In Vivo: The Mouse Model*. New York, NY: Academic Press

Hirano S, Kimoto N, Shimoyama Y, Hirohashi S, Takeichi M (1992) Identification of a neural alpha-catenin as a key regulator of cadherin function and multicellular organization. *Cell* **70**: 293–301

Hoshi O, Ushiki T (1999) Scanning electron microscopic studies on the route of neutrophil extravasation in the mouse after exposure to the chemotactic peptide N-formyl-methionyl-leucyl-phenylalanine (fMLP). *Arch Histol Cytol* **62**: 253–260

Kemler R (1993) From cadherins to catenins: cytoplasmic protein interactions and regulation of cell adhesion. *Trends Genet* **9**: 317–321

Lampugnani MG, Orsenigo F, Gagliani MC, Tacchetti C, Dejana E (2006) Vascular endothelial cadherin controls VEGFR-2 internalization and signaling from intracellular compartments. *J Cell Biol* **174**: 593–604

Ley K, Laudanna C, Cybulsky MI, Nourshargh S (2007) Getting to the site of inflammation: the leukocyte adhesion cascade updated. *Nat Rev Immunol* **7**: 678–689

Majno G, Palade GE (1961) Studies on inflammation. 1. The effect of histamine and serotonin on vascular permeability: an electron microscopic study. *J Biophys Biochem Cytol* **11:** 571–605

Marchesi V (1961) The site of leukocyte emigration during inflammation. *Q J Exp Physiol Cogn Med Sci* **46:** 115–118

Marchesi VT, Gowans JL (1964) The migration of lymphocytes through the endothelium of venules in lymph nodes: an electron microscope study. *Proc R Soc Lond B Biol Sci* **159:** 283–290

Monaghan-Benson E, Burridge K (2009) The regulation of vascular endothelial growth factor-induced microvascular permeability requires Rac and reactive oxygen species. *J Biol Chem* **284:** 25602–25611

Muller WA (2003) Leukocyte-endothelial-cell interactions in leukocyte transmigration and the inflammatory response. *Trends Immunol* **24:** 326–333

Nagafuchi A, Ishihara S, Tsukita S (1994) The roles of catenins in the cadherin-mediated cell adhesion: functional analysis of E-cadherin-alpha catenin fusion molecules. *J Cell Biol* **127:** 235–245

Navarro P, Caveda L, Breciario F, Mandoteanu I, Lampugnani MG, Dejana E (1995) Catenin-dependent and -independent functions of vascular endothelial cadherin. *J Biol Chem* **270:** 30965–30970

Nieminen M, Henttinen T, Merinen M, Marttila-Ichihara F, Eriksson JE, Jalkanen S (2006) Vimentin function in lymphocyte adhesion and transcellular migration. *Nat Cell Biol* **8:** 156–162

Noda K, Zhang J, Fukuhara S, Kunimoto S, Yoshimura M, Mochizuki N (2010) Vascular endothelial-cadherin stabilizes at cell-cell junctions by anchoring to circumferential actin bundles through alpha- and beta-catenins in cyclic AMP-Epac-Rap1 signal-activated endothelial cells. *Mol Biol Cell* **21:** 584–596

Nottebaum AF, Cagna G, Winderlich M, Gamp AC, Linnepe R, Polaschegg C, Filippova K, Lyck R, Engelhardt B, Kamenyeva O, Bixel MG, Butz S, Vestweber D (2008) VE-PTP maintains the endothelial barrier via plakoglobin and becomes dissociated from VE-cadherin by leukocytes and by VEGF. *J Exp Med* **205:** 2929–2945

Nourshargh S, Hordijk PL, Sixt M (2010) Breaching multiple barriers: leukocyte motility through venular walls and the interstitium. *Nat Rev Mol Cell Biol* **11:** 366–378

Ozawa M, Baribault H, Kemler R (1989) The cytoplasmic domain of the cell adhesion molecule uvomorulin associates with three independent proteins structurally related in different species. *EMBO J* **8:** 1711–1717

Ozawa M, Kemler R (1998) Altered cell adhesion activity by pervanadate due to the dissociation of alpha-catenin from the E-cadherin.catenin complex. *J Biol Chem* **273:** 6166–6170

Petri B, Broermann A, Li H, Khandoga AG, Zarbock A, Krombach F, Goerge T, Schneider SW, Jones C, Nieswandt B, Wild MK, Vestweber D (2010) von Willebrand factor promotes leukocyte extravasation. *Blood* **116:** 4712–4719

Schoefl GI (1972) The migration of lymphocytes across the vascular endothelium in lymphoid tissue. A reexamination. *J Exp Med* **136:** 568–588

Taddei A, Giampietro C, Conti A, Orsenigo F, Breviario F, Pirazzoli V, Potente M, Daly C, Dimmeler S, Dejana E (2008) Endothelial adherens junctions control tight junctions by VE-cadherin-mediated upregulation of claudin-5. *Nat Cell Biol* **10:** 923–930

Turowski P, Martinelli R, Crawford R, Wateridge D, Papagiorgiou A-P, Lampugnani MG, Gamp AC, Vestweber D, Adamson P, Dejana E, Greenwood J (2008) Phosphorylation of vascular endothelial cadherin controls lymphocyte emigration. *J Cell Sci* **121:** 29–37

Vestweber D (2007) Adhesion and signaling molecules controlling the transmigration of leukocytes through endothelium. *Immunol Rev* **218:** 178–196

Wegmann F, Petri J, Khandoga AG, Moser C, Khandoga A, Volkery S, Li H, Nasdala I, Brandau O, Fässler R, Butz S, Krombach F, Vestweber D (2006) ESAM supports neutrophil extravasation, activation of Rho and VEGF-induced vascular permeability. *J Exp Med* **203:** 1671–1677

Yamada S, Pokutta S, Drees F, Weis WI, Nelson WJ (2005) Deconstructing the cadherin-catenin-actin complex. *Cell* **123:** 889–901

Yonemura S, Wada Y, Watanabe T, Nagafuchi A, Shibata M (2010) alpha-Catenin as a tension transducer that induces adherens junction development. *Nat Cell Biol* **12:** 533–542

Zarbock A, Allegretti M, Ley K (2008) Therapeutic inhibition of CXCR2 by Reparixin attenuates acute lung injury in mice. *Br J Pharmacol* **155:** 357–364